Technologies and Materials for Renewable Energy, Environment & Sustainability

Influence of Selenium on Physical Properties of ZnTe Thin Films

AIPCP25-CF-TMREES2025-00050 | Article

Influence of Selenium on Physical Properties of ZnTe Thin Films

Zainab Assif Abdullah[1, a)] and Ayad Ahmed Salih[2, b)]

[1]*University of Technology, Baghdad, Iraq.*
[12]*Department of Physics, College of Ibn Al-Haytham, University of Baghdad, Iraq.*

[a)] *corresponding author: Zainab.a.abdulla@uotechnology.edu.iq*
[b)] *ayad.a.s@ihcoedu.uobaghdad.edu.iq*

Abstract. $ZnTe_{1-x}Se_x$ (ZTS) semiconductor thin films at various contents (x = 0.0, 0.1, and 0.2) are deposited on glass substrates kept at room temperature by the thermal evaporation technique with a thickness of 500 nm. This study effects of varying the Se content on the variables influencing ZTS thin-film solar cell properties. XRD analysis reveals that the ZTS thin films' structure is cubic and polycrystalline, with a preferred orientation of (111) at $2\theta \approx 25.25$. The intensities of all the peaks rapidly increase. The crystallinity of the films becomes higher. Grain and crystalline diameters (from 8.46 to 41.25 nm) both increase as the (x) content rises. Furthermore, AFM was applied to studying the morphology. All films were homogeneous and smooth, and the (RMS) roughness of the films increases with increasing (x) content. Consequently, the thin-film crystallite size increases. The optical characteristics were examined using a UV/visible spectrophotometer. These films had a direct gap that shrank as the x content increased, reaching its lowest value of 1.86 eV at x= 0.2.

Keywords: Semiconductor, Glass substrates $ZnTe_{1-x}Se_x$, Thin film, XRD, Optical properties.

INTRODUCTION

Trillium zinc belongs to the group (II-VI) semiconductor materials [1,2]. Selenium zinc is a member of group II-VI semiconductor materials. Group II-VI semiconductors have a broad band gap, with the ZnSe value at ambient temperature being roughly 2.7 eV. In addition to the large band gap[3] Since the two elements are semiconductors, members of the same group, and have a face-centered cubic crystal structure by nature, we can conclude that they have a lot in common. These materials can be made synthetically by evaporating in a vacuum or by chemical vapor deposition (CVD), when alloying the two elements in the proper ratios. In general, there are two primary absorption bands present in both of these materials. The first one is located in the near-ultraviolet spectrum, while the second one is in the infrared, with a wavelength of 400 to 500 nm[4]. Because zinc telluride has a high absorption coefficient (10^3-10^5) cm^{-1} and energy gap type direct ranging (2-2.25) electron volts at ambient temperature, which is directly in the green area of the spectrum, it can be used in optoelectronic applications, for example, solar cell, light-emitted diodes, photodetectors, etc. [1,5]. The crystal structure for ZnTe is a cubic where the lattice parameter an equal to 6.101 Å(1). This substance can be employed in a variety of ways, such as vacuum-induced thermal evaporation, to create thin films[6]. spraying [7] metal-organic chemical vapor deposition (MOCVD)[8] electron beam evaporation[9] Light detectors, solar cells, and light-emitting diodes are just a few of its numerous uses[10,11]. Low-wavelength photodetectors are a significant thin-film application[12,13] To investigate the thin layer, optical and structural equipment were employed [14,15]. It has been demonstrated that doping and annealing zinc trillium results in modifications to the energy gap and a notable reduction in resistance [16]. ZnTeSe QD is the most promising emitter for blue QD-LEDs, although tellurium is thought to induce spectrum broadening and efficiency loss [17].

This work focuses on the effect of Se content (x) on the properties of $ZnTe_{1-x}Se_x$ thin films using the thermal evaporation method and their characterization utilizing structural and optical measurements, and the relationship between these parameters.

MATERIALS AND METHODS

$ZnTe_{1-x}Se_x$ (ZTS) alloys have been created with various concentrations of (x = 0.0, 0.1, and 0.2) and a high purity (99.99%) of zinc, tellurium, and selenium in a (1:1:1) stoichiometric weighed proportion. The product alloy placed into quartz tubes was pressurized with 1×10^{-3} mbar, before being heat treated for 6 hours in an electric oven at 1273 K, where it should be mentioned that the temperature needed for complete alloy solidification was above the ZTS melting temperature, Prior to being pulverized into powder, the alloy was lastly permitted to cool gradually until it reached room temperature for a whole day, according to the phase diagram[18] The thermal evaporation method at a pressure of $4.5\text{x}10^{-5}$ Torr with a deposited rates of 5.1 nm/s were used to deposit the ZTS thin films (500 nm) thick onto glass substrates at room temperature.

All prepared samples have homogeneity, substrate adherence, and crack-free nature, in order to investigate the optical and structural properties of $ZnTe_{1-x}Se_x$ thin films. X-ray diffraction (XRD) and AFM have been used to determine the structure (morphology) of ZnTe, $ZnTe_{0.9}Se_{0.1}$, and $ZnTe_{0.8}Se_{0.2}$ films. A (LabX-XRD-6000 SHIMADZU Japan) with radiation λ = 1.5406 Å Cu (K_α) was used to find (XRD) patterns. After examining the X-ray diffraction of these films, Scherer's Formula was used to determine the crystallite size based on the film thickness [19]:

$$C.S = \frac{0.9\,\lambda}{\beta\cos(\theta)} \tag{1}$$

Where, β (FWHM) represents the diffraction width of the peaks at half maximum. Measured the diffraction peak angle (θ) and the crystallite size (C.S). The following equation is used to get the lattice constant (a) [20].

$$\frac{1}{d^2} = \frac{h^2 + k^2 + l^2}{a^2} \tag{2}$$

Where, (hkl) represent Miller's incident location. The following formula can be used to calculate the micro strain (Ɛ) for produced thin films [21].

$$\varepsilon = \frac{\beta\cos\theta}{4} \tag{3}$$

The ratio of the dislocation line lengths to the crystal volume is known as the density of dislocations (δ). The following can be used to compute it [22].

$$\delta = \frac{1}{(C.S)^2} \tag{4}$$

Measurements of optical transmission between 400 and 1000 nm in wavelength were made in order to calculate the energy gap by using a double-beam spectrophotometer (EMCLAB-61PC, UV-visible) through transmission and absorption spectra covering a wavelength range of 400 to 1000 nanometers, optical properties of the thin film production have been studied. The energy gap (E_g) from the absorption spectra has been determined using the Lambert law and the Tauc equations, respectively [20].

$$\alpha = 2.303\frac{A}{t} \tag{5}$$

$$\alpha h\upsilon = D\,(h\upsilon - E_g)^r \tag{6}$$

The precise value of the constant D, which depends on temperature. r indicates the type of optical transition, hυ indicates the energy magnitude of the incident photons, and α represents the absorption coefficient. Absorption (A) and thickness (t).

Relationships that can be used to calculate optical constants include the extinction coefficient k, the refractive index n, and the reflection R.[23].

$$k = \frac{\alpha\,\lambda}{4\pi} \tag{7}$$

$$n = \left[\frac{4R}{(1-R)^2} - k^2\right]^{1/2} + \frac{(1+R)}{(1-R)} \tag{8}$$

RESULTS AND DISCUSSION

The XRD pattern for $ZnTe_{1-x}Se_x$ (ZTS) thin films with thickness 500 nm with x = 0.0, 01, and 0.2 at room temperature, is shown in Figure 1. The existence of multiple diffraction peaks of (111), (220), (311) and (420) planes indicate the polycrystalline nature of the ZTS films compound with a cubic NaCl structure, with the (111) preferred orientation at $2\theta \approx 25.26^{o}$, and this agrees with the study[18,24]. The dhkl-space and (2θ) of the prominent peaks and the crystallite size (C.S) of the films can be determined using the Scherrer equation for peak (111) which is presented in Table 1. The XRD peaks coincide with those of a cubic crystal structure according to the JCPDS file number 00-015-0746 card standard value and the observed 'd' and '2θ' values are in good agreement with standard 'd' and '2θ' values taken from (JCPDS) card data. From the same Table, we can see that as the (x) content rose and the FWHM fell, the crystallite size grew. When the x content increases, the produced films show a significant shift in peak positions, which may be caused by the modest tension created by the (x) atoms' entry and diffusion into the host material as well as their occupation of places in the ZTS crystal lattice. Additionally, we can see that the intensity rises as the x content does. This is because increased x content causes the film's crystallinity to increase[1,9,22]. Calculations of the micro strain (ε) and dislocation density (δ) revealed that, as the (x) content increased, their values decreased (Table 1) as shown in figure 1. This explains why micro strain and full width at mid-maximum (FWHM) have a positive association, while crystal size has a negative correlation. Since δ is a measure of the quantity of defects in a crystal, lower δ-values indicate higher levels of crystallinity for the films. The dislocation density value found in this work is equal to $0.58x10^{15}$ lines/m^2 for x 0.2 films. The ZTS films produced using this thermal evaporation process have good crystallinity, as confirmed by the modest value of δ achieved in this work.

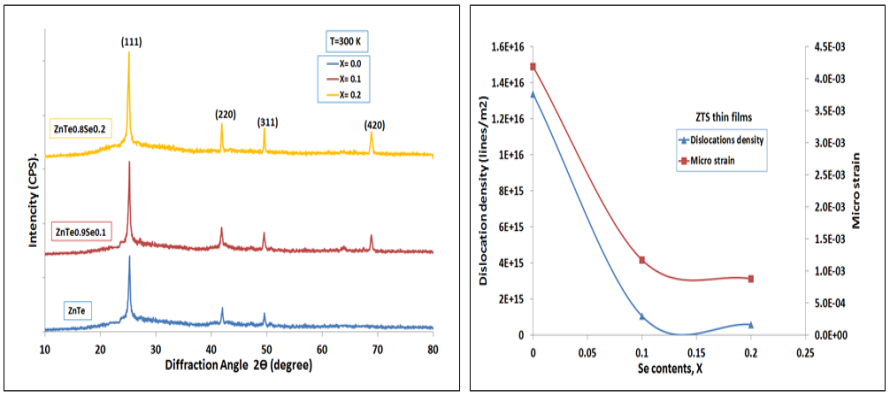

FIGURE 1. Pattern of XRD for ZTS thin films with x= (0.0, 0.1, and 0.2).

TABLE 1. XRD data for ZTS thin films at x = 0.0, 0.1 and 0.2.

(x)	$d_{exp.}$ (Å)	2θexp (deg)	(hkl)	FWHM (deg)	C.S (nm.)	δ × 10^{15} (lines/m^2)	ε × 10^{-3}
ZTS (x= 0.0)	3.5229	25.26	(111)	0.98	8.64	13.37	4.18
	2.1494	42.00	(220)				
	1.8371	49.58	(311)				
ZTS (x= 0.1)	3.5274	25.22	(111)	0.27	30.87	1.04	1.17
	2.1573	41.84	(220)				
	1.8392	49.52	(311)				
	1.3624	68.86	(420)				
ZTS (x= 0.2)	3.5326	25.18	(111)	0.206	41.25	0.58	0.87
	2.1533	41.92	(220)				
	1.8364	49.60	(311)				
	1.3615	68.91	(420)				

Three-dimensional atomic force microscope (AFM) pictures of room-temperature ZTS thin films with different x contents are displayed in Figure 2. Table 2 demonstrates how the root mean square (r.m.s), grain diameter, and surface roughness all raise as the (x) ratio does. As the (x) content increases, we can observe that both the roughness and average diameter rise, which is to be expected given the increase in the Crystals size thin films. We note that the behavior of the grain size (G.S) in the AFM microscope is similar to the behavior of the crystal size (C.S) in the XRD measurements, which confirms the increase in the crystal size with the increase in the Selenium concentration (x) in the films. For ZTS thin films, it was discovered that the greatest values of surface roughness (19.45), root mean square (27.14), and average diameter (78.59) at a doping ratio of (0.2) result in modifications to the film's surface characteristics. The behavior of the $ZnTe_{0.8}Se_{0.2}$ (x=0.2) film data is expected to reduce the reflection of light from its surface, thus increasing the absorption of incident light photons and reducing reflectivity, which makes this film eligible for use in as anti-reflection-coatings or solar cell applications [22,24,25].

TABLE 2. Average roughness, grain size, and (r.m.s) for ZTS thin films at (R.T.)

Thickness (500 nm) (x)	Grain size (nm)	Surfaces roughness (nm)	Root mean square (nm)
ZTS (x = 0.0)	48.36	2.954	3.628
ZTS (x = 0.1)	63.51	9.222	11.50
ZTS (x = 0.2)	78.59	19.45	27.14

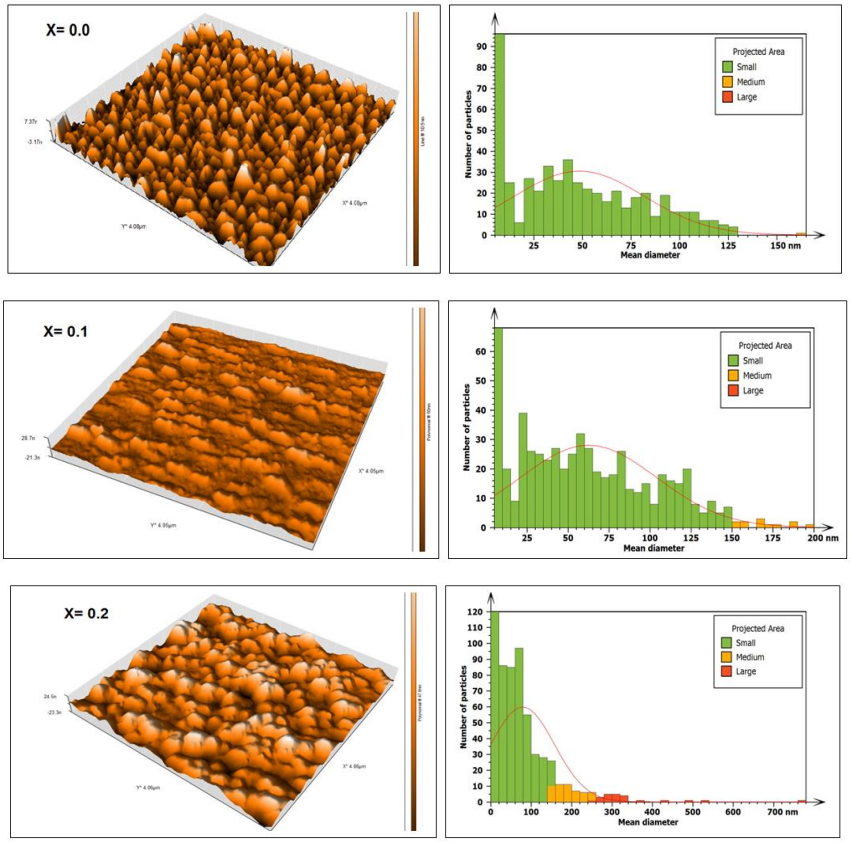

FIGURE 2. 3D AFM micrographs of ZTS thin film

The optical transmittance spectra and absorbance with wavelengths ranging from 400 nm to 1000 nm are displayed in Figure 3. It can be observed that the transmittance of ZTS thin films increases with increasing wavelength, in contrast to absorbance, which decreases with increasing wavelength. As the concentration of (x) increases, the optical transmittance falls; it implies that a higher value of (x) will reduce transparency because free carriers absorb more of it[25]. In the visible spectrum, it is evident that the films are transparent. At wavelengths longer than 550 nm, all of the films exhibit transmittance ranging from 20 to 60%. Nonetheless, the highest transmittance value that falls inside the NIR spectral range surpasses 60%. At the same time, we note from Figure 3 that the absorbance is high in the visible light range, around 90%, and begins to decrease with increasing wavelength. Conversely, as the concentration of (x) increases, the absorbance will increase and the transmittance will decrease. The increase in absorbance is due to the significant surface roughness, which causes light to scatter more. The maximum absorbance value was obtained in the visible band between 400 and 700 nm at a value (x = 0.2) of around 85 to 95%. Below 550 nm, there is a sharp fall in the transmittance of the films, which is due to the strong absorbance of the films in this region. By combining the values of the two diagrams, we find that the reflectivity value will be at its lowest value in the visible light region, and thus, this film can be used in optoelectronic applications.

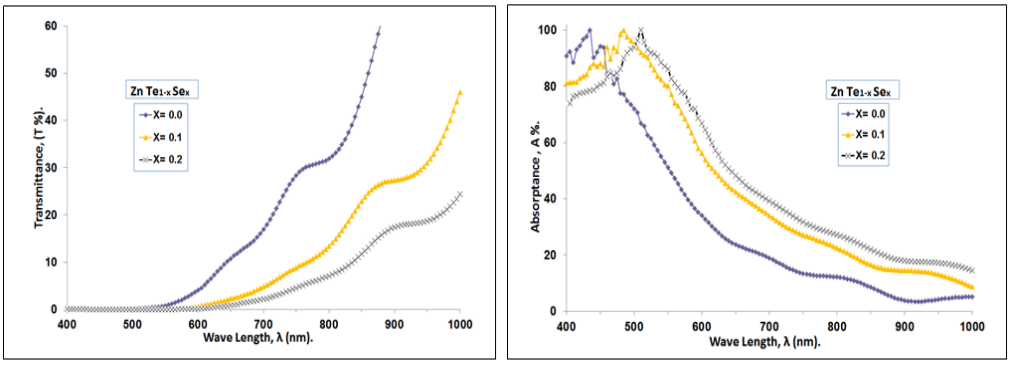

FIGURE 3. The transmittance and absorbance vs. wavelength for ZTS thin films at RT.

Figure 4 illustrates how the (x) ratios affect the ZTS thin film's absorption coefficient and optical energy gap (E_g^{opt}) values in the (400–1000) nm wavelength range. The absorption coefficient of a material indicates how well it absorbs light, and it strongly depends on the photon and band gap energies. The absorption coefficient's α computed values are around 10^4 cm^{-1} and it shows a high value for higher photon energies (shorter wavelengths) in Figurer 4, indicating a high chance of the permitted direct transition and when the wavelength increases, α declines. In addition, we note that as the visible spectrum region is approached, the ZTS thin films' absorption coefficient rises, as seen in Figure 4 and in Table 3. This indicates that the film can be used with solar cell applications. Additionally, it can be shown that absorbance rises sharply close to the band gap edge and increases with increasing (x) concentration. The variation in ZTS film's crystallinity and carrier concentration with (x) concentration may be the cause of this variation. As a result, the absorption edge moved into the long wavelength range and that very clear in Table 3.

The optical band gap energy (E_g^{opt}) was illustrated in Figure 4, Eg was derived from the intercept on the photon energy axis following the extrapolation of the straight-line segment of the curve of $(\alpha h\nu)^2$ versus (hν) plot. It was fond that the energy band gap Eg is influenced by the concentration of (x) with direct band gap is 2.15 eV for pure ZnTe, which is in good agreement with a number of papers[1,26,27]. The film also exhibits direct band transitions, which is a crucial feature for solar applications. The technique used to prepare the film determines whether the shift is toward higher or lower energies[25]. From Table 3 and Figure 4 make it evident that the optical energy gap (Eg) decreases with increasing (x) content, eventually reaching 1.86 eV at 550 nm for x= 0.2. This is to be expected since an increase in the average diameter of ZTS thin films material causes the crystalline size to increase.

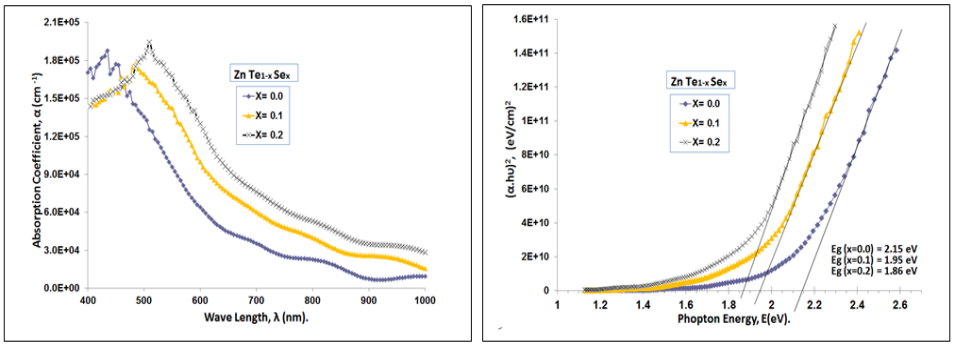

FIGURE 4. The absorption coefficient vs. wavelength & (αhυ)2 vs. photon energy for ZTS thin films at RT.

TABLE 3. The optical parameters of ZTS thin films for λ= 550 nm at (R.T.)

Thickness (500 nm)	E_g^{opt}(eV)	α × 104 (cm-1)	n	k
ZTS (x = 0.0)	2.15	9.59	5.48	0.42
ZTS (x = 0.1)	1.95	14.26	2.3	0.62
ZTS (x = 0.2)	1.86	16.75	1.77	0.73

Some of the electromagnetic radiation that strikes a surface is transmitted, some is absorbed, and some is reflected. The optical constants, which are significant fundamental features of matter, completely characterize the optical behavior of materials [4,21,25] The method of evaporation has a significant impact on the optical characteristics of an evaporated film[25] These optical constants included the extinction coefficient (k), the refractive index (n). Table 3 shows the change in the optical constants of ZTS films at room temperature and at a wavelength of 550, i.e. in the visible spectrum range. Since the refractive index (n) dispersion is a key component of optical communication and the design of devices for spectrum dispersion, it is crucial in the study of optical materials. The films' refractive index values were determined by applying Equation (8). Figure 5 shows that the behavior of the refractive index (n) with λ and the values of n decrease with increase (x) in the visible region due to decrease the corresponding reflection. Additionally, Figure 5 shows that all films exhibit anomalous dispersion when the refractive index drops as the input photon energy increases above the Eg values. The extinction coefficient (k) variation as a function of incident wave length (λ) is displayed in Figurer 5. Since (k) primarily depends on (α) according to Eq. (7), the behavior of (k) is almost identical to that of the corresponding absorption coefficient (α); as a result, we observe that (k) increases with increasing photon energy because the absorption coefficient increases. This indicates that these films have a direct electronic transition [26]. Additionally, it is demonstrated that because of the structural alterations in the films, (k) varies significantly with (x) values of Se.

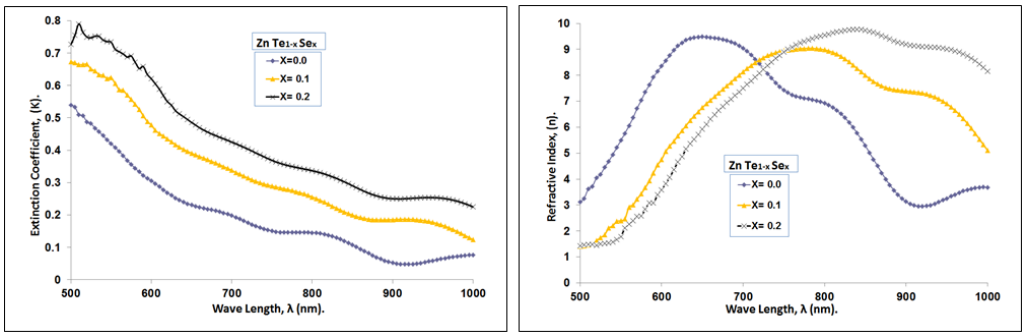

FIGURE 5. The extinction coefficient and refractive index as a function of wavelength for ZTS films at RT

CONCLUSION

$ZnTe_{1-x}Se_x$ (ZTS) thin films were successfully prepared at room temperature using the thermal evaporation process at different contents (x = 0.0, 0.1, and 0.2). The physical characteristics of ZTS thin film were observed to improve with an increase in (x) content. In every film, the XRD showed a polycrystalline cubic structure. The size of the crystallites increased from 8.64 to 41.25 nm as the (x) concentration rose, while the optical gap shrank from 2.15 eV to 1.86 eV. The absorption coefficient also rose from 9.59×10^4 to 16×10^4 cm^{-1} and the refractive index decreases with increasing (x), making them appropriate thin films for solar cells and other various optoelectronic devices.

ACKNOWLEDGMENTS

We thank the Thin Film Lab, Department of Physics / College of Education for Pure Science /Ibn Al-Haitham, University of Baghdad.

REFERENCES

1. Sarmad M. Ali. Fabrication of pure and doped ZnTe/Si heterojunction with Cu using thermal evaporation and study its properties. Baghdad, 2018 Jan.
2. S. M. PATEL AND N. G. PATEL. SWITCHING MECHANISM IN ZnTe FILMS. india; 1984 Jan.
3. Hile DD, Swart HC, Motloung S V, Koao LF. Zinc selenide semiconductor: synthesis, properties and applications. In: Nanoscale compound semiconductors and their optoelectronics applications. Elsevier; 2022. p. 67–84.
4. Palik ED., Ghosh Gorachand. Handbook of optical constants of solids. Coventry, England: Academic Press; 1998. 737–758 p.
5. Rajakarunanayake Y, Cole BH, McCaldin JO, Chow DH, Söderström JR, McGill TC, et al. Growth and characterization of ZnTe films grown on GaAs, InAs, GaSb, and ZnTe. Appl Phys Lett. 1989;55(12):1217–9.
6. Kosasih FU, Erdenebileg E, Mathews N, Mhaisalkar SG, Bruno A. Thermal evaporation and hybrid deposition of perovskite solar cells and mini-modules. Vol. 6, Joule. Cell Press; 2022. p. 2692–734.
7. Gupta A, Parikh V, Compaan AD. High-efficiency ultra-thin sputtered CdTe solar cells. Solar Energy Materials and Solar Cells. 2006 Sep 22;90(15):2263–71.
8. Iwan S, Zhao JL, Tan ST, Sun XW. Enhancement of UV photoluminescence in ZnO tubes grown by metal organic chemical vapour deposition (MOCVD). Vacuum. 2018; 155:408–11.
9. Islam R, Banerjee HD, Rao DR. Structural and optical properties of CdSe,Te,-x thin films grown by electron beam evaporation. Vol. 266, Thin Solid Films. 1995.
10. Patel NG, Panchal CJ, Makhija KK, Patel PG, Patel SS. Fabrication and Characterization of ZnTe/CdSe Thin Film Solar Cells. Vol. 1, Cryst. Res. Technol. 1994 Feb.
11. Mahalingam T, John VS, Rajendran S, Sebastian PJ. Electrochemical deposition of ZnTe thin films. Semicond Sci Technol. 2002;17(5):465.
12. Panaitescu AM, Antohe I, Răduță AM, Iftimie S, Antohe Ștefan, Mihăilescu CN, et al. Morphological, optical, and electrical properties of RF-sputtered zinc telluride thin films for electronic and optoelectronic applications. AIP Adv. 2022 Nov 1;12(11).
13. Hossain MI, Siddiquee K, Islam O, Gafur MA, Qadir MR, Ahmed NA. Characterization of electrodeposited ZnTe thin films. Journal of Optics. 2019; 48:295–301.
14. C. Salame, P. Mialhe, and J.-P. Charles, "VDMOSFET model parameter extraction based on electrical and optical measurements," Microelectron. J. 32, 599–603 (2001).
15. Rajpal S, Kumar SR. Thermoluminescent properties of nanocrystalline ZnTe thin films: Structural and morphological studies. Physica B Condens Matter. 2018; 534:145–9.
16. Tariq GH, Niaz NA, Anis-Ur-Rehman M. EFFECTS OF DOPANT'S PROFILE ON PHYSICAL PROPERTIES OF ZnTe THIN FILMS. Vol. 11, Chalcogenide Letters. 2014.
17. Khudhair, N.H., Jasim, K.A., Preparation and study the effective of Sb on the energy density of states of Se60Te40, AIP Conference Proceedings, 2023, 2769, 020056.
18. . M. Ali SM, Shehab AAA, Maki SA. Effect of Cu doping on the electrical Properties of ZnTe by Vacuum Thermal Evaporation. Ibn Al-Haitham Journal for Pure and Applied Sciences. 2018 Nov 25;31(3):20–5.

19. Salih AA, Mohammed AH, Aneed SH, Hussein BH. Fabrication and Optoelectronic Properties of Bismuth Oxide Thin Films Prepared by Thermal Evaporation. Vol. 20, IRAQI JOURNAL OF APPLIED PHYSICS. 2024.
20. Salih AA, Abad WK, Fadaam SA, Hussein BH. Fabrication of lead oxide nanoparticles by green synthesis method for photovoltaic applications. Dig J Nanomater Biostruct. 2023 Dec 1;18(4):1225–33.
21. Abdulateef, A.N., Alsudani, A., Chillab, R.K., Jasim, K.A., Shaban, A.H., Calculating the mechanisms of electrical conductivity and energy density of states for Se85Te10Sn5-xInx glasses materials, Journal of Green Engineering, 2020, 10(9), pp. 5487–5503.
22. Salih AA. The Structural and Surface Morphology Properties of Aluminum Doped CdO Thin Films Prepared by Vacuum Thermal Evaporation Technique. Ibn Al-Haitham Jour for Pure & Appl Sci [Internet]. 2014 Sep 8;27 (2):1–13. Available from: https://www.researchgate.net/publication/284456533
23. Aleabi, S.H., Watan, A.W., Salman, E.M.-T., kareem Jasim A.,Shaban, A.H., Alsaadi, T.M., The study effect of weight fraction on thermal and electrical conductivity for unsaturated polyester composite alone and hybrid, AIP Conference Proceedings, 2018, 1968, 020019.
24. Ahmed, B.A., Mohammed, J.S., Fadhil, R.N., ...Shaban, A.H., Al Dulaimi, A.H., The dependence of the energy density states on the substitution of chemical elements in the Se6 Te4-xSbx thin film, Chalcogenide Letters, 2022, 19(4), pp. 301–308.
25. Salih AA. The Optical Properties of Aluminum Doped CdO Thin Films Prepared by Vacuum Thermal Evaporation Technique. Ibn Al-Haitham Jour for Pure & Appl Sci [Internet]. 2014;27 (3). Available from: https://www.researchgate.net/publication/284456385
26. Abbas M, Shah NA, Jehangir K, Fareed M, Zaidi A. Physical properties of ZnTe semiconductor thin films prepared by high vacuum resistive system. Materials Science- Poland. 2018;36(3):364–9.
27. Vázquez-Barragán NE, Olvera-Rivas R, Marasamy L, Quinones-Galvan JG, Santos-Cruz J, Guillen-Cervantes A, et al. Optoelectronic properties of undoped and N-doped ZnTe films grown by RF sputtering: Effect of the substrate temperature and N nominal concentration. Materials Science and Engineering: B. 2023; 296:116695.